Electronic supplementary information (ESI) for:

Elucidation of Structural Features and Photoluminescence Properties for Hydrothermally-synthesized γ-$KEu(MoO_4)_2$ Microcrystal Phosphor with Metastable Orthorhombic Structure and Differences of Luminescence Properties by Structure Transition Due to Y^{3+}-dilution

Takuya Hasegawa,[a,†] Suzuka Noda,[a] Wataru Hikita,[b] Kenji Toda,[b] Ayahisa Okawa[a] and Shu Yin[a,c]

[a] *Institute of Multidisciplinary Research for Advanced Material (IMRAM), Tohoku University*
[c] *Graduate School of Science and Technology, Niigata University*
[c] *Advanced Institute for Materials Research (WPI-AIMR), Tohoku University*

†Corresponding author:

Dr. Takuya Hasegawa

Tel/Fax +81-22-217-5598, E-mail: hase@tohoku.ac.jp

Contents

1. **Table S1** Results of elemental analysis by XPS for KEM-HT and KEM-SSR
2. **Table S2** Atomic parameters refined by Rietveld analysis: KEM-HT and KEM-SSR
3. **Table S3** Structural and atomic parameters optimized by DFT calculation: α-KEu$(MoO_4)_2$ and γ-KEu$(MoO_4)_2$
4. **Figure S1** The SAED patterns of KEM-HT and KEM-SSR
5. **Figure S2** Comparison of PL spectra under various excitation bands of (blue) CTS and (red) $^7F_0 \rightarrow {}^5L_6$ transition of Eu^{3+}: (A) KEM-HT and (B) KEM-SSR phosphors.
6. **Figure S3** Contour plots of the temperature-dependent PL spectra of the (A) KEM-HT and (B) KEM-SSR. (C) Temperature dependency of the PL peak intensity for the KEM-HT and KEM-SSR.
7. **Figure S2** Spin-considered partial and total DOSs of γ-KEu$(MoO_4)_2$: (top) up-spin and (bottom) down-spin
8. **Figure S3** Spin-considered partial and total DOSs of α-KEu$(MoO_4)_2$: (top) up-spin and (bottom) down-spin

Table S1 Results of elemental analysis by XPS for KEM-HT and KEM-SSR

Samples	Components / at%		
	K	Eu	Mo
KEM-HT	22.35	23.33	54.32
KEM-SSR	24.89	20.83	54.28

Table S2 Atomic parameters refined by Rietveld analysis: KEM-HT and KEM-SSR

KEM-HT

Atom	Wyckoff	Occ.*	x	y	z	Ueq.** (Å^2)
Mo1	8d	1	0.5213(5)	0.10259(8)	-0.0165(3)	1.38(6)
Eu1	4c	1	0	0.0073(1)	0.25	0.61(6)
K1	4c	1	0.5	0.2700(3)	0.25	2.4(2)
O1	8d	1	0.742(2)	0.0967(9)	0.157(2)	0.5
O2	8d	1	0.753(2)	0.0864(9)	-0.196(2)	3.8(5)
O3	8d	1	0.254(2)	0.0330(5)	-0.011(3)	0.1(3)
O4	8d	1	0.394(2)	0.1874(5)	-0.023(2)	2.1(4)

* Occ.: site occupancy; ** Ueq.: isotropic temperature factor

KEM-SSR

Atom	Wyckoff	Occ.	x	y	z	Ueq. (Å^2)
Eu1	2i	1	-0.0678(6)	0.116(1)	0.2338(9)	0.5
Mo1	2i	1	0.1762(7)	0.633(2)	0.250(1)	0.5
Mo2	2i	1	0.7166(7)	0.636(2)	0.277(1)	0.5
K1	2i	1	0.425(2)	0.096(4)	0.219(3)	0.5
O1	2i	1	0.236(3)	0.821(7)	0.074(6)	0.5
O2	2i	1	0.322(3)	0.565(7)	0.407(5)	0.5
O3	2i	1	0.063(3)	0.789(7)	0.363(5)	0.5
O4	2i	1	0.061(3)	0.221(7)	0.032(6)	0.5
O5	2i	1	0.575(3)	0.287(7)	0.107(5)	0.5
O6	2i	1	0.639(3)	0.861(7)	0.451(6)	0.5
O7	2i	1	0.893(3)	0.572(7)	0.418(5)	0.5
O8	2i	1	0.693(2)	0.824(7)	0.096(6)	0.5

Table S3 Structural and atomic parameters optimized by DFT calculation: α-$KEu(MoO_4)_2$ and γ-$KEu(MoO_4)_2$

KEM-HT					
Orthorhombic			Space group: *Pbcn* (60)		
a (Å)	5.064564		α (°)	90	
b (Å)	17.746437		β (°)	90	
c (Å)	7.864813		γ (°)	90	
V ($Å^3$)	706.873416				
Atom	Wyckoff	Occ.	x	y	z
Mo1	8d	1	0.5	0.267272	0.25
Eu1	4c	1	0	0.008044	0.25
K1	4c	1	0.51692	0.104155	0.97919
O1	8d	1	0.727607	0.106238	0.158903
O2	8d	1	0.741204	0.097224	0.802551
O3	8d	1	0.25353	0.032989	0.004661
O4	8d	1	0.378985	0.192858	0.974072

KEM-SSR					
Triclinic			Space group: $P\bar{1}$ (2)		
a (Å)	11.10395		α (°)	112.6113	
b (Å)	5.202171		β (°)	111.9007	
c (Å)	6.797244		γ (°)	91.45358	
V ($Å^3$)	329.7078				
Atom	Wyckoff	Occ.	x	y	z
Eu1	2i	1	0.555987	0.873101	0.750152
Mo1	2i	1	0.061835	0.871111	0.75129
Mo2	2i	1	0.823478	0.366168	0.748041
K1	2i	1	0.284219	0.351266	0.716701
O1	2i	1	0.799853	0.251384	0.946652
O2	2i	1	0.678621	0.441227	0.586036
O3	2i	1	0.91295	0.135642	0.59429
O4	2i	1	0.934455	0.711827	0.91892
O5	2i	1	0.410167	0.645212	0.898326
O6	2i	1	0.339659	0.10054	0.527838
O7	2i	1	0.129621	0.45519	0.567619
O8	2i	1	0.254584	0.186828	0.88685

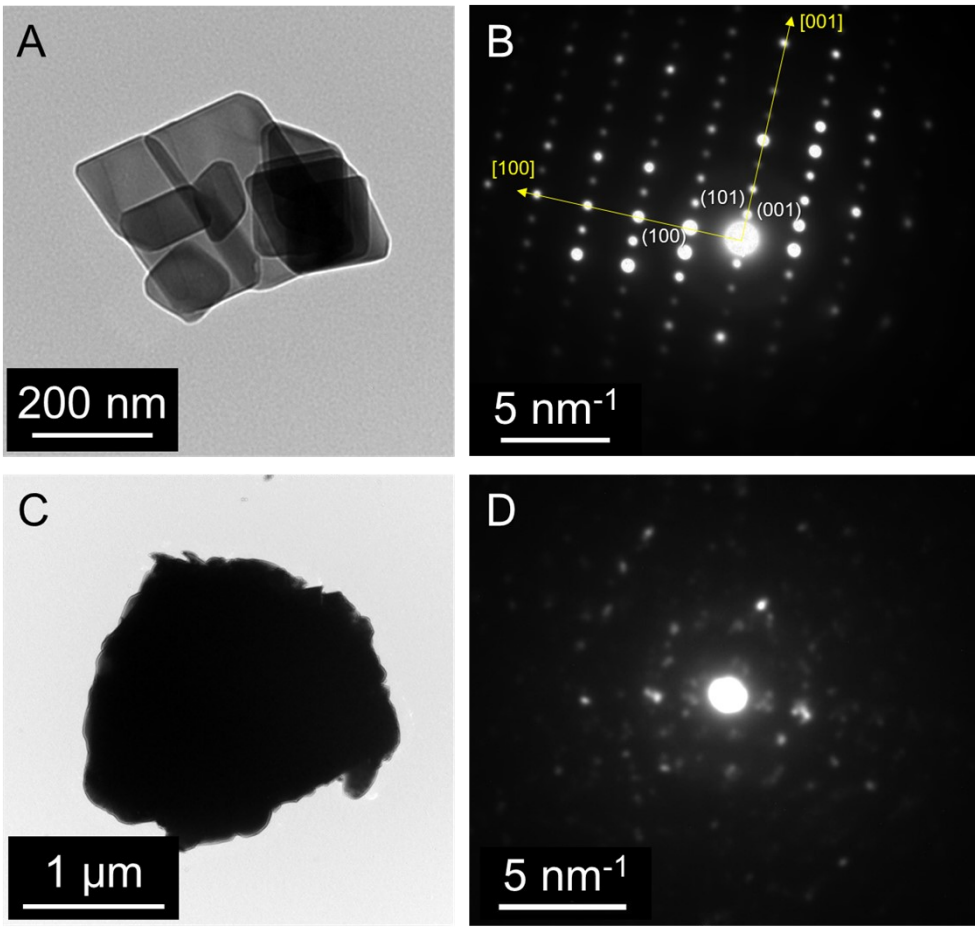

Figure S1 The SAED patterns of KEM-HT and KEM-SSR

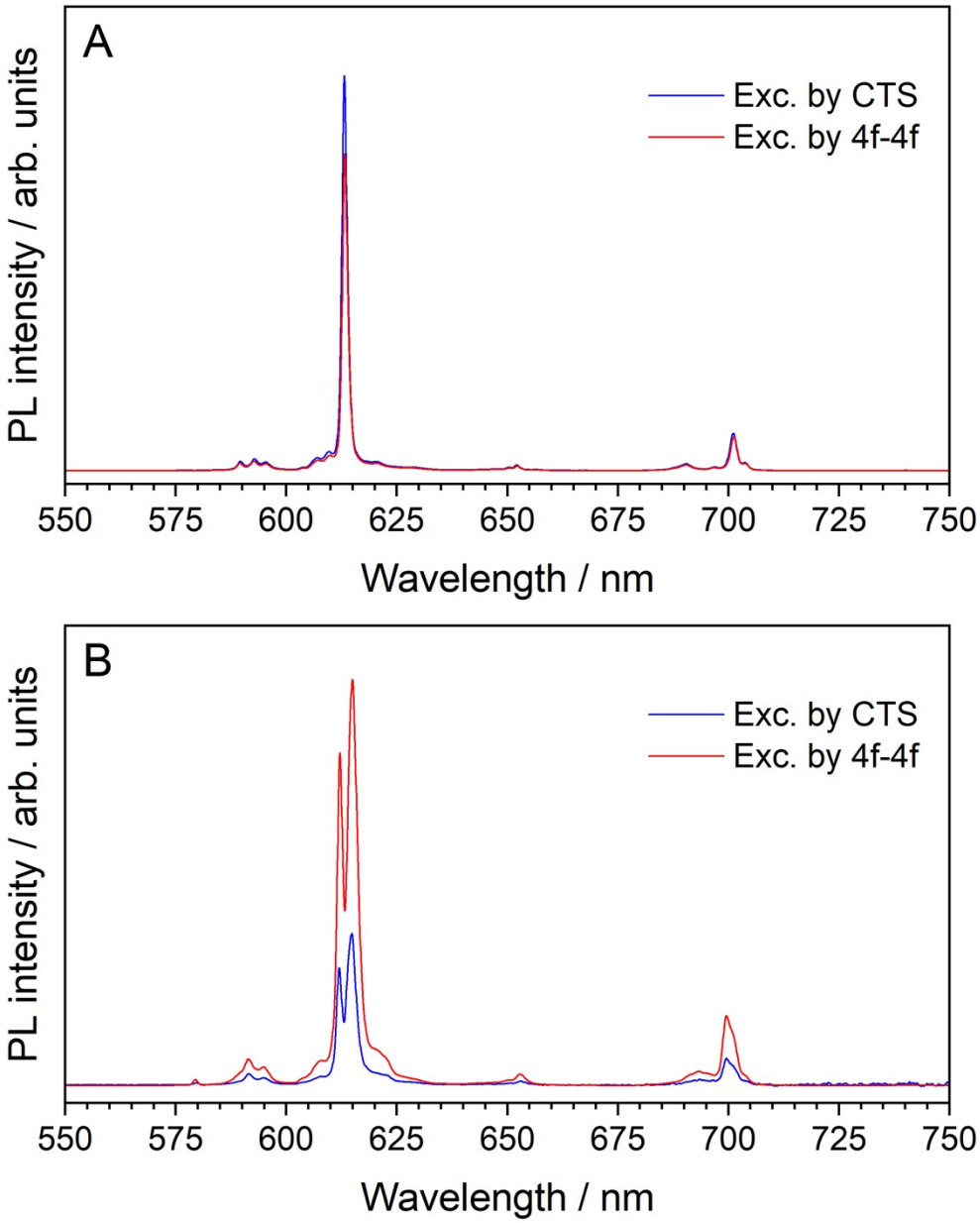

Figure S2 Comparison of PL spectra under various excitation bands of (blue) CTS and (red) $^7F_0 \rightarrow {}^5L_6$ transition of Eu^{3+}: (A) KEM-HT and (B) KEM-SSR phosphors.

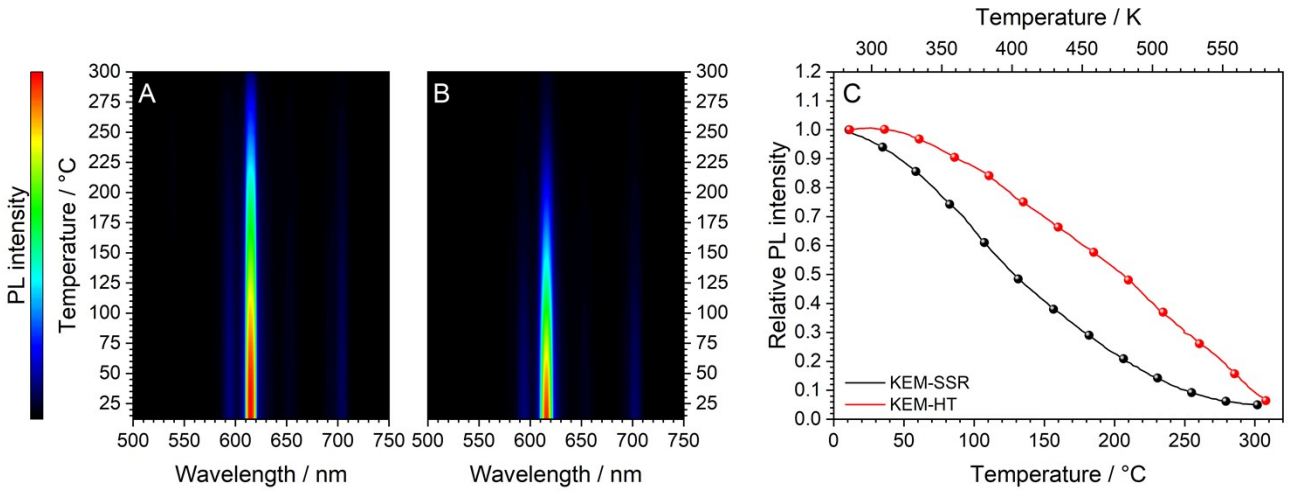

Figure S3 Contour plots of the temperature-dependent PL spectra of the (A) KEM-HT and (B) KEM-SSR. (C) Temperature dependency of the PL peak intensity for the KEM-HT and KEM-SSR.

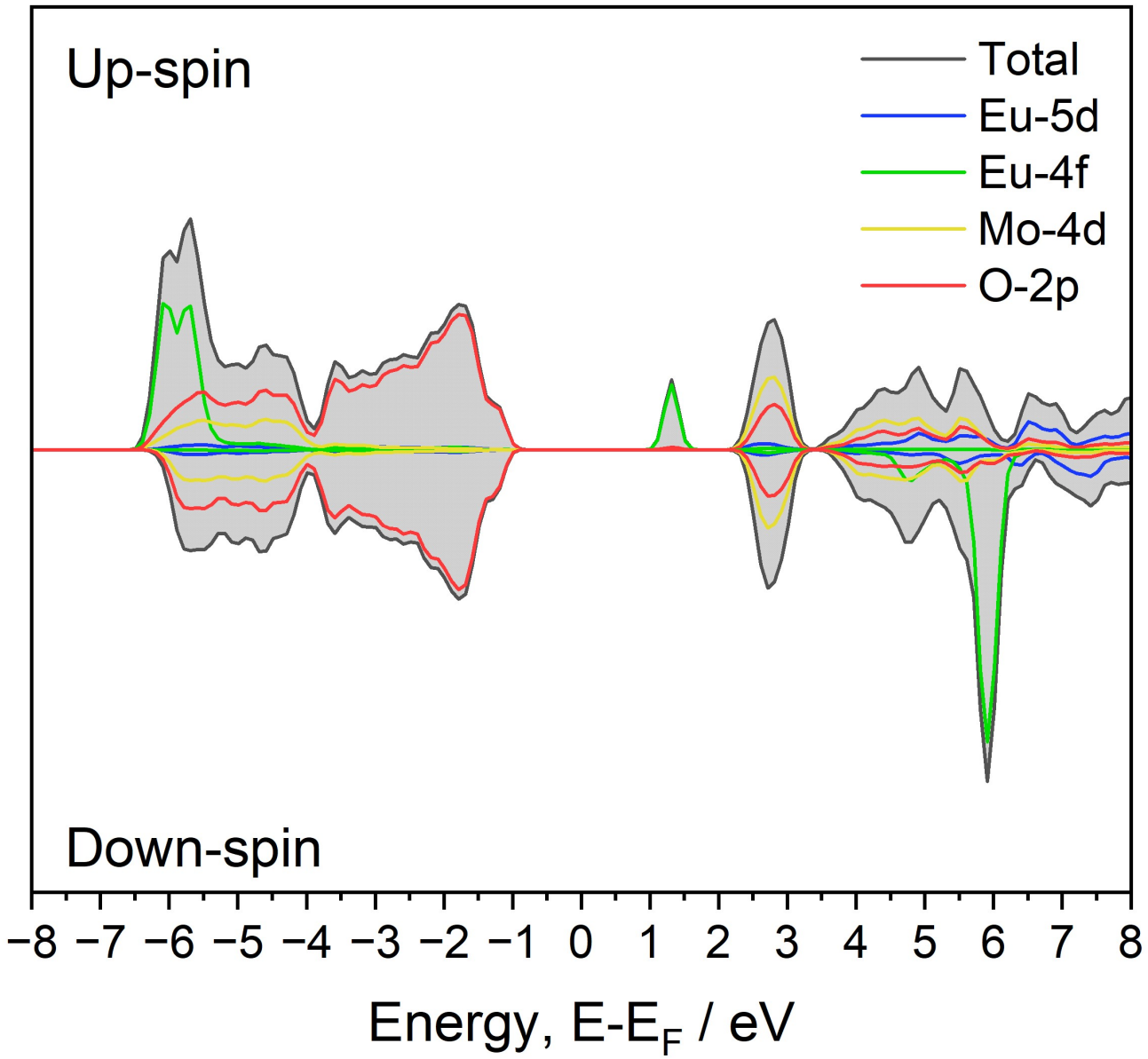

Figure S4 Spin-considered partial and total DOSs of γ-$KEu(MoO_4)_2$: (top) up-spin and (bottom) down-spin

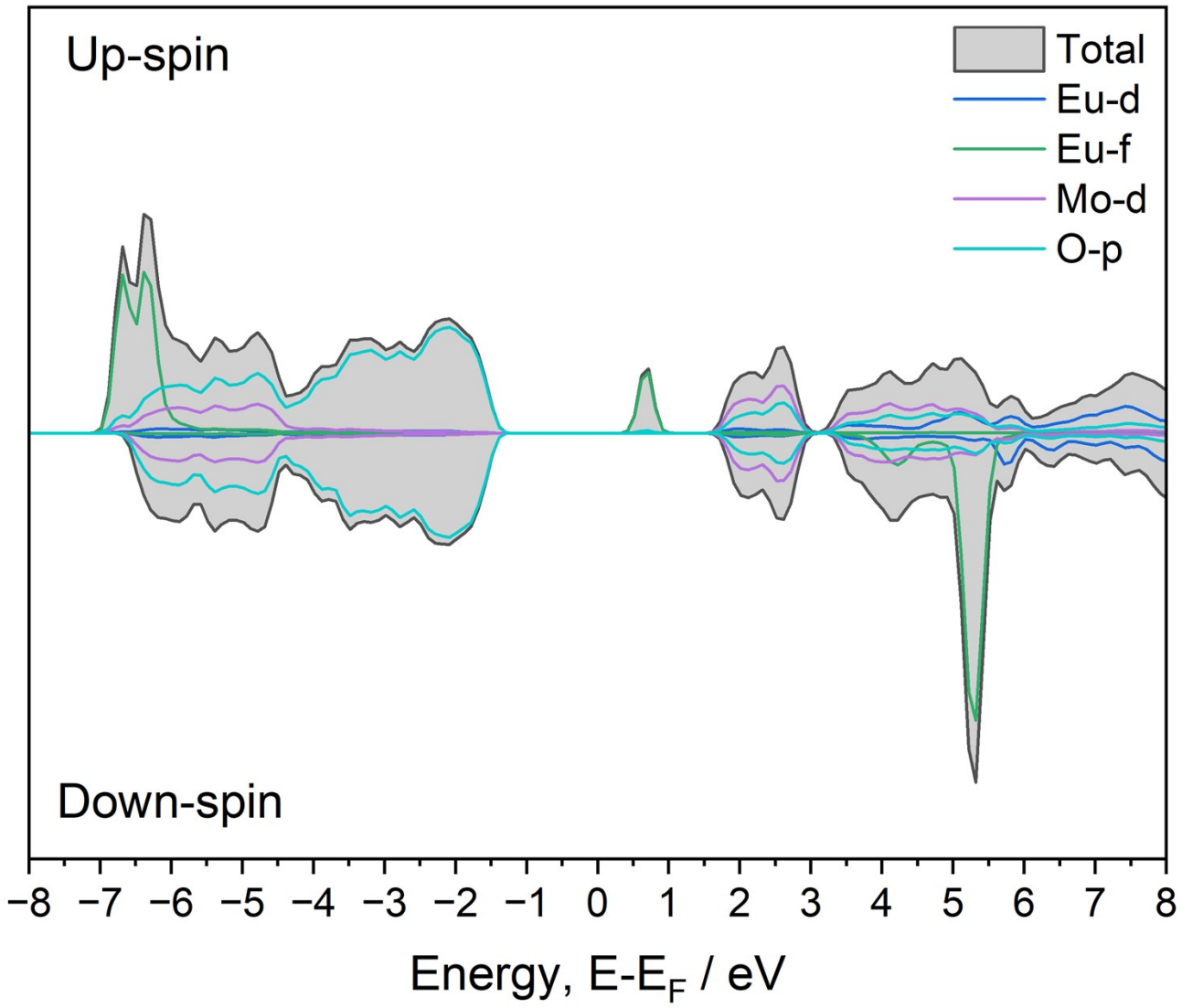

Figure S5 Spin-considered partial and total DOSs of α-$KEu(MoO_4)_2$: (top) up-spin and (bottom) down-spin